Heliyon 9 (2023) e18452

Contents lists available at ScienceDirect

Heliyon

journal homepage: www.cell.com/heliyon

# Improving single-hand open/close motor imagery classification by error-related potentials correction

Yanghao Lei [a,b], Dong Wang [a,b], Weizhen Wang [a,b], Hao Qu [a,b], Jing Wang [a,b,*], Bin Shi [c,**]

[a] Institute of Robotics and Intelligent System, School of Mechanical Engineering, Xi'an Jiaotong University, Xi' an,710049, China
[b] Research Institute of NRR-Neurorehabilitation Robot, Xi' an Jiaotong University, Xi' an,710049, China
[c] PLA Rocket Force University of Engineering Xi'an, Xi' an, 710025, China

ARTICLE INFO

*Keywords:*
Brain computer interface
Motor imagery
Error-related potentials
Electroencephalogram
Correction strategy

ABSTRACT

*Objective:* The ability of a brain-computer interface (BCI) to classify brain activity in electroencephalograms (EEG) during motor imagery (MI) tasks is an important performance indicator. Because the cortical regions that drive the single-handed open and closed tasks overlap, it is difficult to classify the EEG signals during executing both tasks.

*Approach:* The addition of special EEG features can improve the accuracy of classifying single-hand open and closed tasks. In this work, we designed a hybrid BCI paradigm based on error-related potentials (ErrP) and motor imagery (MI) and proposed a strategy to correct the classification results of MI by using ErrP information. The ErrP and MI features of EEG data from 11 subjects were superimposed.

*Main results:* The corrected strategy improved the classification accuracy of single-hand open/close MI tasks from 52.3% to 73.7%, an increase of approximately 21%.

*Significance:* Our hybrid BCI paradigm improves the classification accuracy of single-hand MI by adding ErrP information, which provides a new approach for improving the classification performance of BCI.

## 1. Introduction

The brain-computer interface (BCI) eliminates the direct influence of nerves and muscles around the limbs and builds a direct pathway for information interaction between the brain and the external environment [1]. Electroencephalography (EEG) is a noninvasive electrical signal that can be easily obtained from the brain. BCI technology provides a new way for patients with intact nervous systems but physical disabilities to manipulate the external world. EEG-based BCI has the advantages of high temporal resolution, safety, and portability. It can be applied to a variety of tasks, including but not limited to neurofeedback [2], restoring motor function in patients with paralysis [3], interacting with patients at risk of communication disorders [4], improving sensory processing [1], and controlling external devices such as robotic arms [5]. Decoding motor intent from brain optisignals is a core problem in achieving these functions. Several paradigms have recently been established for EEG-based BCI to extract a user's motor intent,

* Corresponding author. Institute of Robotics and Intelligent System, School of Mechanical Engineering, Xi'an Jiaotong University, Xi' an,710049, China.
** Corresponding author.
*E-mail addresses:* wangpele@gmail.com (J. Wang), sb902580@stu.xjtu.edu.cn (B. Shi).

https://doi.org/10.1016/j.heliyon.2023.e18452
Received 14 July 2022; Received in revised form 15 July 2023; Accepted 18 July 2023
Available online 20 July 2023

including error-related potentials (ErrP) [6], motor-related cortical potentials (MRCP) [7], motor imagery (MI), and motor execution (ME) [8].

The MI and ME paradigms have significant performance in decoding the user's motion intention, especially the motion of different lateral limbs (e.g., left/right hand and upper/lower). The areas corresponding to cortical activation during the execution or imagining of similar movements of the ipsilateral limb are close to or even overlap with each other [9], making the recognition of motor intent for similar movements more difficult. Current researchers have improved the decoding accuracy by using higher-density channels of EEG signals, more sophisticated preprocessing and classification algorithms, and classification of ME signals with more differentiated movements of different limbs. Liao et al. used high-density 128-channel recordings of ME signals and extracted the corresponding power spectrum features to decode ten pairs of finger movements (e.g., index finger to thumb, index finger to middle finger) within the same hand to obtain 77.1% accuracy [10]. Deng et al. applied a time-frequency synthesized spatial pattern BCI Algorithm [11] and a classifier-enhanced time-frequency synthesized spatial pattern algorithm [12]to 163 channel EEG signals of motion execution to classify the torque intentions of the elbow and shoulder. In the healthy subjects, the accuracies were 89% and 100%, respectively. Chakraborti et al. controlled the motion of a robot by classifying six types of ME signals from the fingers-shoulders-elbows on both sides of the limbs, with 87%, 67.5%, 68.39%, and 70.12% classification accuracy for the left and right limbs, elbows, fingers, and shoulders [13]. Because patients with motor function hemiplegia cannot control the injured limbs to perform motor tasks, it is not feasible to use ME signals to decode similar movements of the same limbs for neurological rehabilitation. The MI paradigm allows patients with motor function hemiplegia to voluntarily imagine rather than perform an action and to achieve neuromodulation rehabilitation by providing rewards through virtual reality or external robots performing the corresponding tasks. Owing to the limitations ossf the low spatial resolution and signal-to-noise ratio (SNR) of MI signals, MI-based BCI systems are extremely challenging to decode different MI tasks with similar body positions of the same limb. Similar movements of the ipsilateral limbs, such as hand opening and closing, assume important functions in life, and decoding hand movements by MI signals is important for hand rehabilitation training in stroke patients. The current dichotomous classification of MI signals for single-hand open and closed movements is slightly higher than that of the random level [14]. Aleksandra and Francisco classified four different movements of the right wrist (extension, flexion, pronation, and supination), obtaining a classification accuracy of 58–82% [15]. The accurate recognition of MI signals for different hand movements can provide finer control for external devices. However, the accuracy of decoding similar hand motions using MI signals is low and needs to be improved urgently. Furthermore, the classification performance is highly dependent on EEG signal processing, especially advanced feature learning methods.

Event-related potentials (ERPs) provide an important method for studying the human mind and brain, and the stability and performance of BCI systems, such as the P300-speller systems [16,17], can be improved by detecting ERPs. Error-related potentials (ErrPs) is an ERP resulting from the perception of erroneous behavior, characterized by an error between 50 and 100 ms after the events of the central EEG shows negative waves in the time domain, and is called a false negative potential ($N_E$); then, the error between 200 and 500 ms after the incident on the top area of the brain electrical signal in the time domain expression is a positive wave and is called false positive potential ($P_E$) [18]. Similar to other ERPs, the ErrP is time-locked. Depending on the three types of error, there are three different types of ErrPs. When people need to make quick choices in a task, errors will occur. The latency of the negative wave is approximately 100 ms. This type of ErrP is called interactive ErrP. When people obtain the feedback state in the task, if the feedback state is wrong, the ErrP is called the feedback ErrP, and the latency is 250 ms. The third type of ErrP is called observation ErrP, which occurs when people find the occurrence of task execution errors in the process of observing the agent to perform tasks with a latency of 250 ms [19]. The ErrP of the paradigm proposed in this article belongs to feedback ErrP.

Methods to improve system robustness by automatically detecting ErrP in a BCI have been widely accepted by researchers. ErrP has been successfully applied to BCI based on sensorimotor rhythms (SRM) and ERPs. ErrP was used to identify and correct errors during the task execution. Bhattacharyya et al. used MI and P300 EEG signals to locate the position of the robotic arm and ErrP to correct the position deviation, which increased the average target attainment rate to 95% and improved the accuracy of the robotic arm movement execution [20]. Ciabattoni et al. added ErrP detection to a wheelchair system to reduce the rate of obstacles in semi-autonomous navigation and improve the safety of the system [21].

The combination of ErrP and MI is typically used to correct errors in MI tasks by determining whether there are errors after MI. This inspired us to conduct this article, the main contributions of this article are as follows: 1). In this article, a hybrid paradigm was

**Table 1**
Demographics of 11 subjects.

| Subjects | Age | Gender | Handedness |
|---|---|---|---|
| 1 | 22 | Male | Right-handed |
| 2 | 23 | Male | Right-handed |
| 3 | 25 | Male | Right-handed |
| 4 | 24 | Male | Right-handed |
| 5 | 25 | Male | Right-handed |
| 6 | 24 | Male | Right-handed |
| 7 | 24 | Male | Right-handed |
| 8 | 24 | Male | Right-handed |
| 9 | 23 | Female | Right-handed |
| 10 | 22 | Female | Right-handed |
| 11 | 23 | Female | Right-handed |

proposed to introduce ErrP into the single-hand MI experiment. The introduction of ErrP added new information to the MI process. The classification accuracy of MI was improved by detecting ErrP. To further improve the accuracy two correction strategies were proposed in the article. 2). EEG data from 11 healthy subjects were validated and the experimental results showed the superior performance of the proposed method.

The article is structured as follows. Section 2 introduces the specific details of the method. Section 3 analyses the experimental results. Section 4 discusses the current work. And section 5 is the conclusion.

## 2. Method

### 2.1. Participants

Eleven healthy subjects (eight males and three females, all right-handed, mean age $\pm$ SD $=$ 23.5 $\pm$ 1.1years) without neurological disorders participated in this study. The demographic details of each participant's age, sex, and handedness are listed in Table 1. All subjects signed an approved informed consent form before participating. All subjects were informed of the purpose and experimental process before the recording of the EEG. This study was approved by the Ethics Committee of Xi'an Jiaotong University.

### 2.2. Paradigm

In this article, we propose a novel hybrid BCI paradigm based on ErrP and MI, as shown in Fig. 1. In each run, a dark screen was first displayed for 2s, followed by a white cross for 2s. Subjects were asked to relax on a dark screen and paid attention when a white cross was displayed. An audio cue of "hand open" or "hand closed" was then played to tell the participant the MI task, while an image cue indicating hand movement for 2 s was played (fist to palm for hand open MI task and palm to fist for hand closed MI task). The probability of the hand opening cue was set at 50%. After receiving the cue, subjects imagined the initial gesture of the action execution (the fist gesture was the initial gesture for the hand opening action). Afterward, the paradigm displayed the image of the fist or palm feedback for 1s to elicit ErrP. When the picture feedback was different from the imagined feedback, the subject realized that the feedback was incorrect and ErrP was generated. The probability of error occurrence was set to 40%. After a short "di" sound cue, a video of the hand opening or closing was played for 3 s. The hand open/closed in the video corresponded to 6–7 s of image feedback, and if the image feedback was the fist to palm, the video would be displayed with the hand open. During this period subjects performed the previous 4–6s audio and image cues of the MI task. When the error occurred, the subjects actually performed a different MI task with the video task, and we denoted such an MI task a negative MI (Ne MI) task. When errors did not occur, subjects performed the same MI task as the video task, and we denoted such an MI task as a Positive MI (Po MI) task. At the end of the trial, an emoji was displayed for 2 s, allowing the subjects to blink and rest. The subjects were instructed not to blink at other times to reduce electro-oculographic artifacts from the EEG signals. Subjects performed two tasks in a single trial: the first task was the ErrP task in 6–7s and the second task was the MI task in 7–10s. The ErrP and MI tasks were randomized during the experiment, and the feedback image was the first frame of a video clip from the same trial. A trial lasted 12s. Each subject had a total of 20 runs, with each run containing 10 trials lasting 120 s. The participants had a short rest period between each run.

When the paradigm is running, the label of MI task (MI Label) and the label of video task (Video Label) are recorded and the label of Ne MI (Ne Label) is determined. When the MI task is Ne MI, Ne Label will be set to 1, which means this trail has error feedback. When the MI task is Po MI, the Ne Label will be set to 0, which means there is no error feedback for this trail.

### 2.3. Data acquisition

The experiment was conducted in a quiet room with the subject comfortably seated in an armchair, 70 cm from the display. The paradigm was displayed on a VOC screen at a refresh rate of 60 Hz. The subjects were asked to watch the screen and avoid body and eye moving during the task.

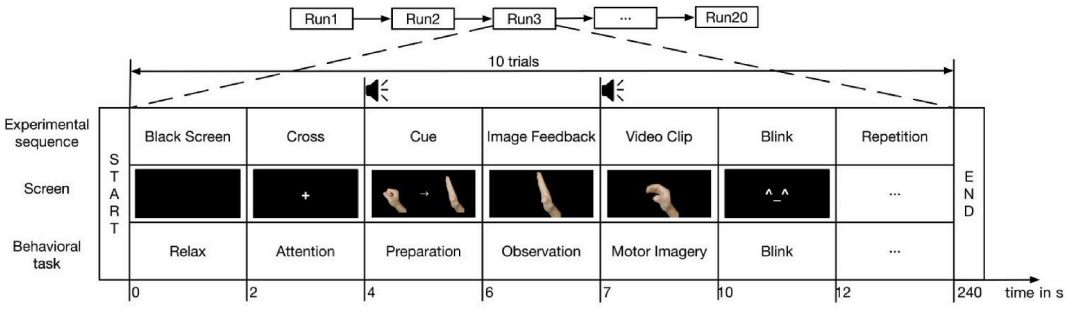


**Fig. 1.** A hybrid BCI paradigm based on ErrP and MI is proposed in this article. The cue for Preparation is presented with a 50% probability of hand open and closed. The image feedback during observation and the video clip during MI appear different (error) with a 40% probability. There are voice prompts before the Preparation and MI.

In previous ErrP studies, EEG was usually acquired on Fz, FCz, CPz, and Cz [19]. In MI studies, electrodes are usually chosen from the C3 and C4 of the motor cortex [22]. Sixteen electrodes (F1, Fz, F2, FC3, FC1, FCz, FC2, FC4, C3, C1, Cz, C2, C4, CP1, CPz, and CP2) in the International 10-10 system were adopted in the experiments, as shown in Fig. 2. The EEG was collected using a g.USBamp (g.tec, Austria) system with a sampling rate of 1200 Hz. Signals were referenced to a unilateral earlobe and grounded in another earlobe. An online notching filter (48–52) Hz was utilized to remove power line interference. The impedance of all electrodes was kept below 5kΩ during the experiment. The presentation of the paradigm was controlled using Psychophysics Toolbox 3.0.

### 2.4. Extract of MI ErrP

ErrP is usually expressed in the form of a difference wave, which is obtained by subtracting the potential for correct task execution from the potential for error task execution in the same time window [23]. This article also used this expression to obtain the difference wave by subtracting the potential of correct feedback from the potential of error feedback and then drew three curves in the same picture. The collected EEG data were filtered at 4–10 Hz which contains the θ-band (4–7 Hz). The filter used was a fourth-order Butterworth filter.

### 2.5. Extract of MI ERD

The ERP phenomenon mainly manifests as a change in the energy amplitude of signals at different frequencies. When the human brain is engaged in thinking activity, it leads to an increase in the amplitude of certain frequency bands of EEG signals, a phenomenon known as Event-related Synchronization (ERS). In contrast, when the human brain performs thinking activities, it also decreases the amplitude of certain frequency bands of EEG signals, a phenomenon known as event-related desynchronization (ERD). Active thinking of the human brain, limb movement processes, and simple motor imagination without performing movement can lead to ERD and ERS phenomena, so the frequency amplitude changes of EEG signals during different motor imaginations can be studied as a theoretical basis for brain-computer interface technologies.

There are many methods to calculate the ERD. The sliding window energy [24] was used in this article. Assume that $X_{ch}^{k}(t)$ is the EEG signal of the *ch*th channel at moment *t* after the 4th order 8–30 Hz Butterworth bandpass filtering of the original signal, where *k* indicates the data for the *k*th EEG segment under the hand opening or closing motor imagery task. Firstly, the square of the signal amplitude was calculated according to equation (1).

$$Y_{ch}^{k}(t) = X_{ch}^{k}(t)^{2} \tag{1}$$

Then, a window of 1s was taken to slide over each point to calculate the average value as the energy $P_{ch}^{k}(t)$ at the current point according to equation (2).

$$P_{ch}^{k}(t) = \frac{1}{N}\sum_{t-0.5}^{t+0.5} Y_{ch}^{k}(t) \tag{2}$$

where: *N* represents the number of sampling points in the time window.

Calculation of the average energy during the baseline according to equation (3).

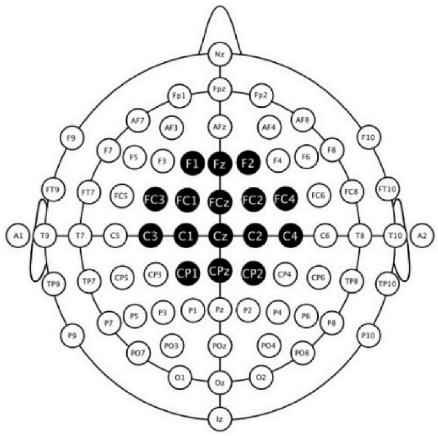


**Fig. 2.** The location of the 16 selected electrodes in the International 10-10 system. 64-electrode system using international 10–20 standard. Reproduced with permission from http://www.mariusthart.net/downloads/eeg_electrodes_10-20.svg, ©Marius 't Hart - http://www.beteredingen.nl.

$$P_{ch}^{k}(t) = \frac{1}{L}\sum_{t=t_0}^{t=t_1} P_{ch}^{k}(t) \tag{3}$$

where $t_0$ and $t_1$ represent the moments before and after the baseline, respectively, and L represents the number of sampling points during the baseline period.

The percentage change in energy is then calculated according to equation (4).

$$ERD_{ch}^{k}(t) = \frac{P_{ch}^{k}(t) - R_{ch}}{R_{ch}} \times 100\% \tag{4}$$

Finally, the energy values were superimposed and averaged according to hand opening and closing to obtain ERD curves of the contralateral energy of the brain motor areas over time.

### 2.6. Classification

The raw data of each subject were filtered and segmented to obtain signals for 200 trials each during the ErrP and MI tasks. For ErrP tasks, data from 0.2 s before and 0.5 s after the occurrence of an error (image feedback) are captured as sample data. The final data format was a three-dimensional matrix with a size of 200 × 16 × 840. Among them, there were 80 trails of image feedback and gestures for the opposite case of the MI movement. In order to eliminate the influence of sample size imbalance in machine learning, data enhancement technique was used to expand it to 100 trails of data through interpolation (Wang et al., 2021). For the MI task, data were obtained from 3s EEG signals during the video clip, and the final data format was 200 × 16 × 3600. Among them, there were 100 trails of MI hand opening. Firstly, the acquired EEG data were filtered to 4–30 Hz using a fourth-order Butterworth filter to extract the ErrP and ERD of the MI. The common average reference was then applied to the data to further improve the SNR of the EEG data.

Owing to the highly structured form of EEG data, many machine learning methods and pattern recognition algorithms have been applied to the classification of EEG signal data in recent years [25]. Some new machine-learning algorithms have been shown very powerful classification performance [26,27]. This article uses pre-processed EEG data as input features for training and classification using convolutional neural networks (CNN). The CNN architecture used in this article is an improvement inspired by reference [28]. Fig. 3 shows the CNN architecture used in this article to classify ErrP and MI signals. A CNN consists of five main layers: an input layer, two convolutional layers, a fully connected output layer, and an output layer. The network architectures for classifying ErrP and MI data are almost the same, with a slightly adjusted convolutional kernel. The input layer of the CNN has dimensions of $N_{ch} \times N_{fc} \times 1$, where $N_{ch}$ represents the number of channels and $N_{fc}$ represents the number of samples. This layer performs a 1D convolution on the channel dimension (Nch). The first convolutional layer kernel of the CNN for classification ErrP was $N_{ch} \times 24 \times 1$, and the first convolutional layer kernel of the CNN for classification MI was $N_{ch} \times 30 \times 1$. The goal of this layer is to learn to weigh the contribution of each channel differently. The number of convolutional kernels in the Conv_1 layer was two and four, and the dimensionality of each feature map was 1 × 409 and 1 × 51, respectively. The Conv_2 layer operates based on the spectral representation of the input. The kernel dimensions of this layer for the two CNNs are 1 × 4 × 2 and 1 × 12 × 4 respectively. The numbers of convolutional kernels in this layer were one and eight, respectively. The outputs of layers Conv_1 and Conv_2 were normalized. Normalization has been shown to reduce the internal covariance within the input samples, resulting in samples with zero average and unit variance [29], which, in turn, improves the generalization performance and training speed of the neural network [30]. The output layer of the network consists of two units corresponding to both the hand open/closed tasks. The output layer is equipped with a softmax function to output the probability of a given input segment belonging to a specific class.

The statistical results of this article were analyzed by paired *t*-test and repeated measure ANOVA. These statistical test methods were calculated by using SPSS 24.0 mathematical tool. All methods were implemented with MatlabR2021b on a computer (3.2 GHz CPU, R7-5800H, 16 GB RAM).

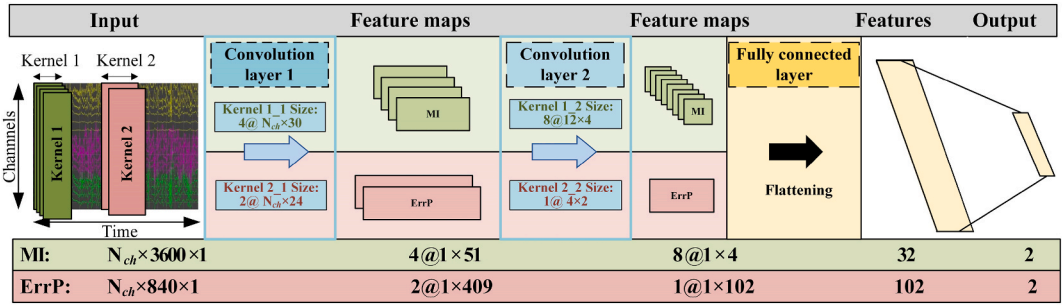


**Fig. 3.** CNN architecture of ErrP and MI. CNN is composed of five layers, an input layer, two convolutional layers, a fully connected layer, and an output layer. The kernel parameters of the convolution layer are different for ErrP/MI classification tasks. Kernel 1 (including Kernel 1_1 and 1–2) represents the convolution kernel for classifying MI. Kernel 2 (including Kernel 2_1 and 2-2) represents the convolution kernel for classifying ErrP.

### 2.7. Correction strategy

For the classification of the CNN, which is a 2-class MI classification, the result is compared with the actual motion MI labels to determine whether the classification is correct. The hybrid paradigm proposed in this article used different classification strategies to obtain different results. In addition to classifying MI directly by CNN, the MI task could be inferred by detecting ErrP. We used image feedback and video clips as labels (video Label) to infer MI tasks (Fig. 4). During the experiment, if ErrP was detected, we assumed that the subject performs the MI task in the opposite direction of the motion in the video clip.

After obtaining the MI classification result (MI Result) of the CNN, we used correction strategies to correct it and used it as the final classification result (Corr Result). Our correction strategies uses image feedback and video clips as labels (Video Label) in the hybrid paradigm proposed in this article to correct the classification result of the CNN. During the experiment, if ErrP was detected, we corrected the MI Result to be the opposite task of the Video Label. The following two correction strategies are proposed in this article:

1. ErrP Corr MI: The correction strategy for correcting MI classification results using ErrP is: if the ErrP signal is detected, the MI task performed by the subject is considered the opposite of the video action task, and it will be treated as a correction result. If ErrP is not detected, the MI task performed by the subject is considered the same as the video action task, and the video label will be used as the correction result. The four classification results for different video motions (where ErrP was considered to be detected) were then corrected. Two incorrect classification results were corrected and the other two correct classification results were retained. Fig. 5 shows the correction cases for the hand-open MI task using the ErrP classification result. For the case in which the MI task is hand open, the video task is hand closed, and the image feedback is also hand closed, there are four MI and ErrP classification results. In the case of incorrect MI classification results (Fig. 5 (a) and (b)), the MI results are corrected to the right classification results once ErrP is detected. In the case of correct MI classification results (Fig. 5 (c)), the accuracy of the classification results is not affected by whether ErrP is detected or not.
2. Ne Corr MI: The classification label of ErrP is Ne Label, and we further use Ne Label to correct the MI classification results. The correction strategy is: as long as the Ne Label recorded in the paradigm running is 1, the task opposite to the Video Label is used as the correction result. The correction strategy is shown in Fig. 6 (see Algorithm 1 for the calculation procedure). The classification accuracy is significantly improved after correction using this strategy. For hand opening and closing MI, the classification results of the CNN corresponded to eight different cases when the MI task and the picture feedback/video clip presented the same (Po) and different (Ne) motions. Compared with the classification results before correction, the number of corrected results has increased and the classification accuracy has improved.

## 3. Results

### 3.1. ErrP and MI ERD

Fig. 7 shows the optimal performance of the single-subject average ErrP features of all the subjects in the four channels Fz, FCz, CPz, and Cz. The average ErrP features of each participant (Fig. 7 S1–S11) were observed. After EEG signal processing, all Po and Ne trials were averaged and got difference wave (diff) from Ne minus Po. Subject 11 (Fig. 7 S11) exhibited the most obvious ErrP features in the Fz channel. The Ne signal showed a large negative wave at approximately 250 ms, and the negative wave began to decline from 200 ms, while the Po signal only fluctuated slightly. Due to individual differences among subjects, ErrP occurred at different times, but they all occurred at about 0.2s to 0.4s after the feedback of wrong images. The scalp distribution of ErrP was then analyzed. With correct image feedback, the overall distribution of activated areas in the cerebral cortex of subject 4 was relatively stable (Fig. 8a), while the error state showed a spatial distribution and a temporal change in voltage amplitude reduction for multiple electrodes from 300 ms to 350 ms (Fig. 8b). Subject 4 had negative wave production in the vicinity of Cz and Fz channels, with more features (blue areas) produced in the anterior half of the brain compared to other regions, which is the same result obtained in previous studies where error-related potentials were concentrated in the midline channels of the brain [6]. The reason for having negative wave features in large areas of the prefrontal lobe is the overall correlation of brain signals and the prefrontal lobe itself is a brain region associated with

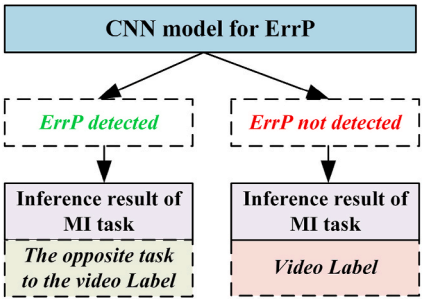


**Fig. 4.** Using ErrP detection results to infer MI tasks. If ErrP is detected, we use the task opposite to Video Label as the inference result of the MI task.

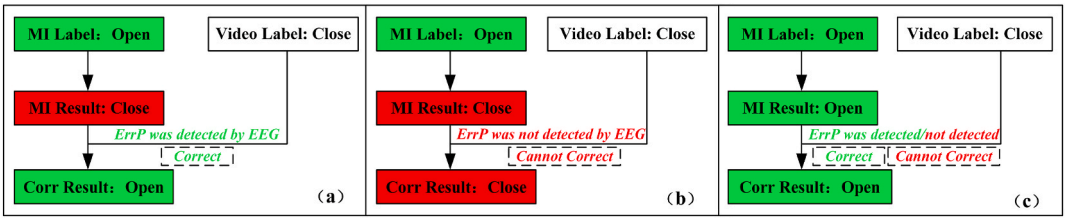


**Fig. 5.** Three cases of using the ErrP Corr MI strategy to correct hand-open MI tasks. Red blocks indicate incorrect classification results and green blocks indicate correct classification results. In the case of Ne MI task, the wrong MI result can be corrected to the correct result if ErrP is detected (a), and cannot be corrected if ErrP is not detected (b), and the correction method does not change the correct MI result (c). (For interpretation of the references to colour in this figure legend, the reader is referred to the Web version of this article.)

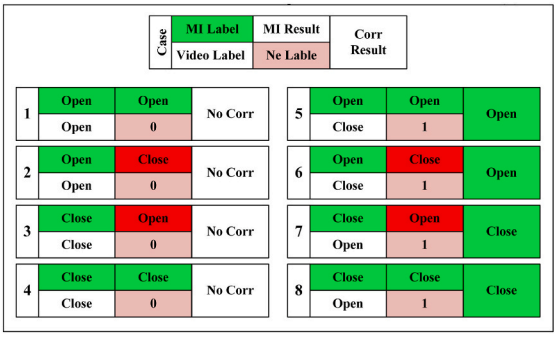


**Algorithm 1:** Correction strategy logic

**input :** *MI Result*, *Ne Label*, *Video Label*
**output:** *Corrected MI Result*

```
if Ne Label = TRUE then
    if Video Label = Open then
    Corrected MI Result ← Close;
    if Video Label = Close then
    Corrected MI Result ← Open;
else
    Corrected MI Result ← MI Result;
end
```

**Fig. 6.** Eight cases of using the Ne Corr MI strategy to correct MI results. The block in red colour is the wrong result, block in green colour is the right and correction result, and block in brown colour is Ne Label. Six of these cases will get the correct classification result. (For interpretation of the references to colour in this figure legend, the reader is referred to the Web version of this article.)

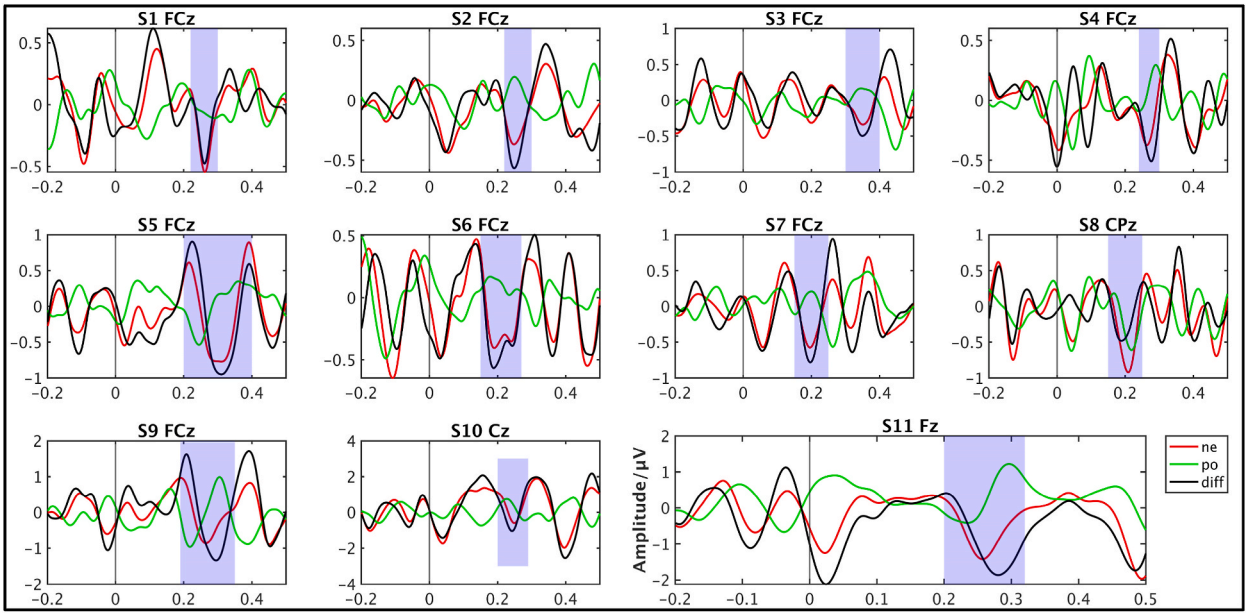


**Fig. 7.** The optimal performance of the single subject average ErrP features of all subjects in the four channels Fz, FCz, CPz, and Cz. ($p < 0.05$). Time 0 ms corresponds to the start of Image Feedback. Ne generates a negative wave from 200 ms and has a large negative wave at about 250 ms, while Po only fluctuates slightly.

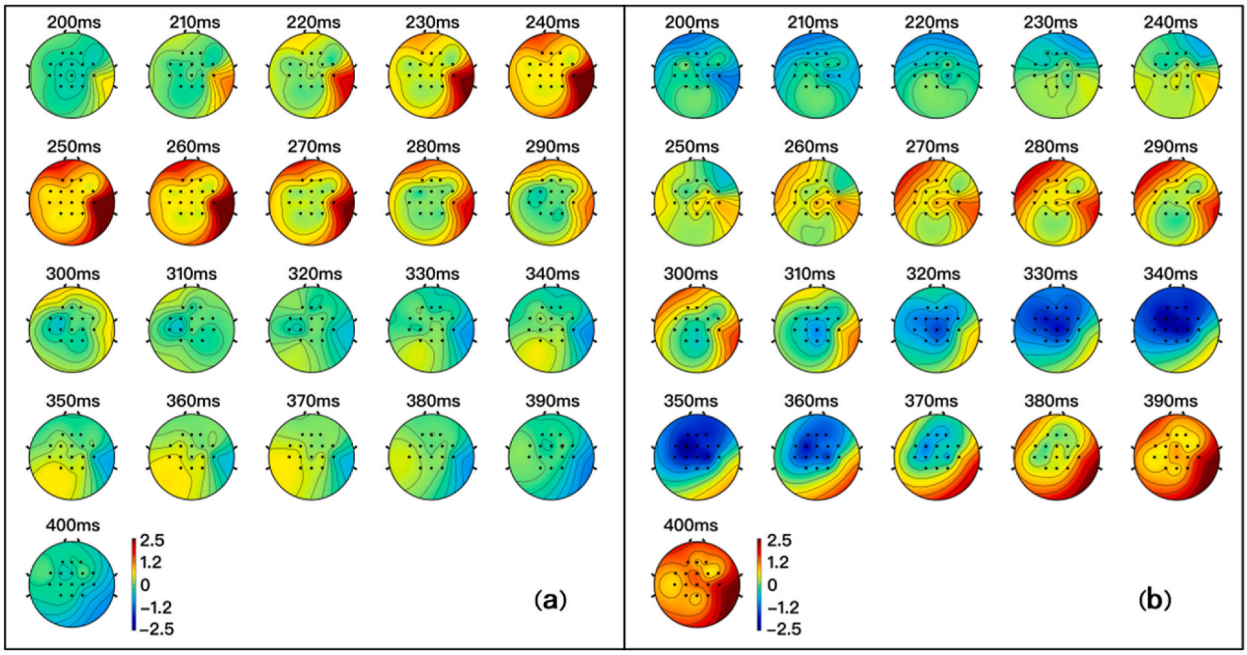


**Fig. 8.** Grand-averaged topographical distribution of subject 4 during the image correct feedback (a) and the error feedback (b). Red represents ERS and blue represents ERD. (For interpretation of the references to colour in this figure legend, the reader is referred to the Web version of this article.)

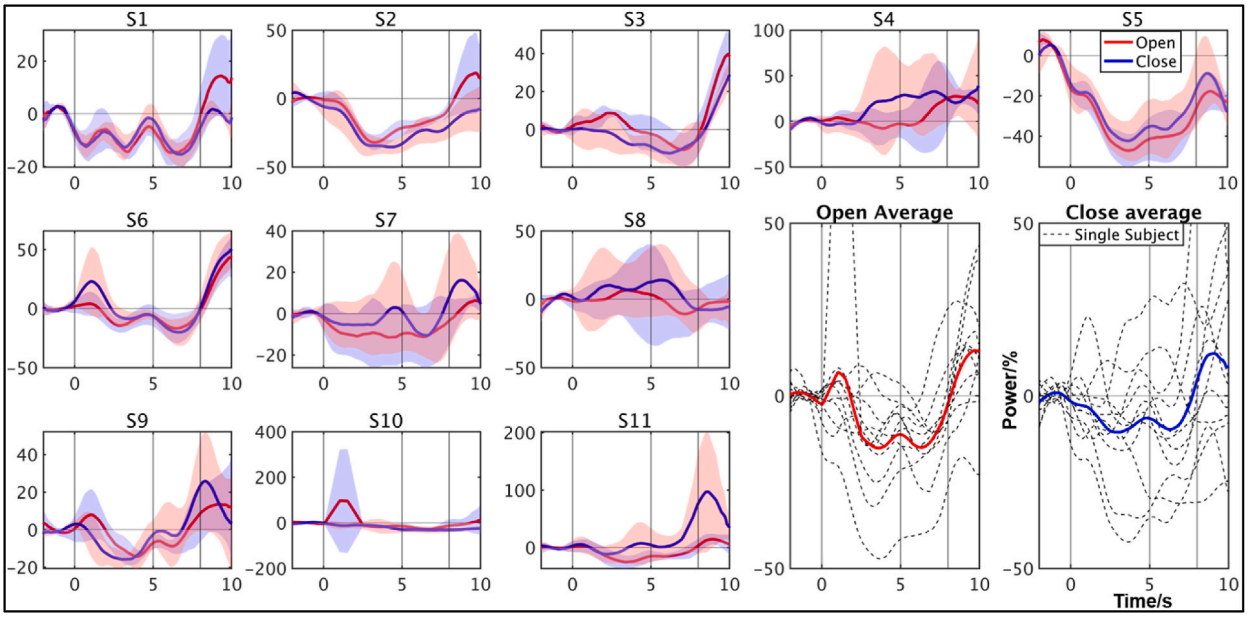


**Fig. 9.** The average MI ERD in 8–30Hz of C3 channels for all subjects in the hand open/close MI tasks. Time 0 corresponds to the beginning of the experiment (the 2 nd s in the paradigm), and time 5 (the 7th second in the paradigm) corresponds to the beginning of the video clip. A significant ERD occurs around time 5s.

cognition.

Fig. 9 shows the average band power ERD of the C3 channel for all subjects (S1–S11) in the hand-open and hand-closed MI tasks. The ERD in the EEG signals of most individual subjects was significant, and the average ERD for all subjects was retained. For both hand-open and hand-closed, the average ERD of all subjects showed ERD phenomena during the beginning phase of the experiment (0s to 5s) and again significantly at the beginning of the MI task (5s).

### 3.2. Classification accuracy

Each subject's data were classified using the built CNN neural network. Classification results were obtained for five different methods. In the experimental paradigm described in Section 2.1, the probability of error occurrence was set to 40%. Among the 200 groups of data collected by each subject, 120 were MI data and 80 were ErrP data.

The first method uses the data enhancement technique mentioned in section 2.6 to expand the same MI task test (Po MI) data from 120 video clips into 200 trails of Po MI data for classification. The second method is to classify 200 MI task trials (Po + Ne MI). The third method is to classify 200 ErrP tasks and infer MI tasks using the method described in subsection 2.7. The fourth and fifth methods use ErrP Corr MI and Ne Corr MI methods described in subsection 2.7 to correct the classification results of Po + Ne MI, respectively. For five cases, the first 100 task data collected from each subject's experiment were used to train the model, and the last 100 task data were used to test the model. Table 2 and Fig. 10 show the accuracy of the five cases for all the subjects.

The Ne Corr MI accuracy was above 70%, the Po + Ne MI accuracy was above 60%, and the Po MI accuracy and Po + Ne MI accuracy were slightly higher than 50%. Compared with Po MI, Po + Ne MI had an average improved accuracy of 9.1%, and Ne Corr MI had an average improved accuracy of 21.3%. Ne Corr MI had the best classification performance in S10 (82%), an improvement of 29% compared with Po MI. For ErrP detection, the accuracy was approximately 63% and the ErrP Corr MI accuracy was approximately 55%. Fig. 11 shows the average accuracy for all cases. A repeated measures ANOVA was conducted on the classification accuracy of 11 healthy subjects under the 5 classification methods, and the Greenhouse-Geisler estimate of deviation from sphericity was w = 0.57, with significant differences between the 5 classification results ($F(2.29,22.9)=177.583$, $p<0.0001$, bias $\eta^2=0.95$). Multiple comparisons showed that Ne Corr MI classification accuracy was significantly higher than Po MI classification accuracy ($t(40)=14.76$, $p<0.001$,$d=21.1$), Po + Ne MI classification accuracy ($t(40)=1.56$, $p<0.001$,$d=3.21$), ErrP classification accuracy ($t(40)=-8.2$, $p<0.001$,$d=-20.7$), and ErrP Corr MI classification accuracy ($t(40)=12.14$, $p<0.001$,$d=15.4$).

In terms of binary classification of MI signals from single-hand open/close motion, the accuracy of Po MI was improved by 10.9% from 52.3% to 63.1% using the classification results of ErrP to infer MI tasks (ErrP). This means that new information contained in ErrP can help MI obtain higher classification accuracy. After the introduction of ErrP (ErrP Corr MI), the accuracy of Po MI increased from 52.3% to 55.3%, which indicates the effectiveness of this correction strategy. This result will be further improved when ErrP has a higher classification accuracy. It should be noted that in the case that the ErrP classifier identifies the EEG during the correct feedback as ErrP and the MI classification result is correct, the correction result will be incorrect and reduce the MI classification accuracy. The proposed correction strategy Ne Corr MI can further improve the classification accuracy based on the introduction of ErrP, and the classification accuracy can be improved by up to 25% in S8. This indicates that the correction strategy has a significant impact on the classification accuracy and can improve the classification accuracy of MI from the original random level to higher separability. This method can be introduced into other difficult MI tasks to improve classification accuracy.

To evaluate the classification performance, we used two baseline models based on support vector machine (SVM) in the MI-based BCI study: CSP+SVM [31] and FBCSP+SVM [32]. Table 3 shows the performance of CNN compared to traditional methods for classifying ErrP and Po MI ($p<0.0001$). The results show that there are significant differences between the comparison and the CNN models. The classification results of the CNN showed a good and stable performance for all subjects.

## 4. Discussion

In the case of Ne Corr MI, the classification accuracy improved by 29% in subject 10. However, the accuracy in the ErrP-Corr MI case was only improved by 5%. Different ErrP accuracies will result in different accuracies of ErrP Corr MI. In addition, the accuracy of Po + Ne MI and the number of Ne labels can cause different correction accuracies. For ErrP accuracy, if we remove the trials that we don't think are Ne trials in the Ne-labelled trials and remove the trials that don't think are Po trials in the Po-labelled trials, and use the remaining data for training and classification, we can achieve an accuracy rate of over 75%. Previous studies [33]have taken out trails with insignificant characteristics. When the trained model was used to classify the entire dataset without removing any data, the accuracy was still only approximately 62%. Because we informed the subjects to cooperate with the experiment, we finally decided to use the entire data for training and classification. If other methods can be used to improve the classification accuracy of ErrP, the ErrP-Corr MI results can be improved.

Owing to the introduction of new features at different times, there are other classification schemes for this paradigm. By combining the ErrP two-class classification during the ErrP task and the MI two-class classification during the MI task, a four-class classification can be achieved. In addition, during the MI task, there are two kinds of hand open and closed MI in correct and error, which can be classified into four categories. Similarly, during the ErrP task, there are two kinds of Po and Ne in hand open and closed MI, which also

**Table 2**
Classification accuracy of different cases of all subjects.

| | S1 | S2 | S3 | S4 | S5 | S6 | S7 | S8 | S9 | S10 | S11 | Average |
|---|---|---|---|---|---|---|---|---|---|---|---|---|
| Po MI | 52 | 53 | 55 | 50 | 53 | 55 | 51 | 50 | 52 | 53 | 52 | 52.3 |
| Po + Ne MI | 62 | 63 | 62 | 58 | 60 | 61 | 62 | 62 | 58 | 66 | 62 | 61.4 |
| ErrP | 67 | 62 | 64 | 61 | 62 | 64 | 59 | 62 | 66 | 62 | 65 | 63.1 |
| ErrP Corr MI | 57 | 55 | 55 | 54 | 56 | 55 | 54 | 54 | 54 | 57 | 57 | 55.3 |
| Ne Corr MI | 70 | 71 | 74 | 74 | 72 | 75 | 71 | 75 | 73 | 82 | 73 | 73.7 |

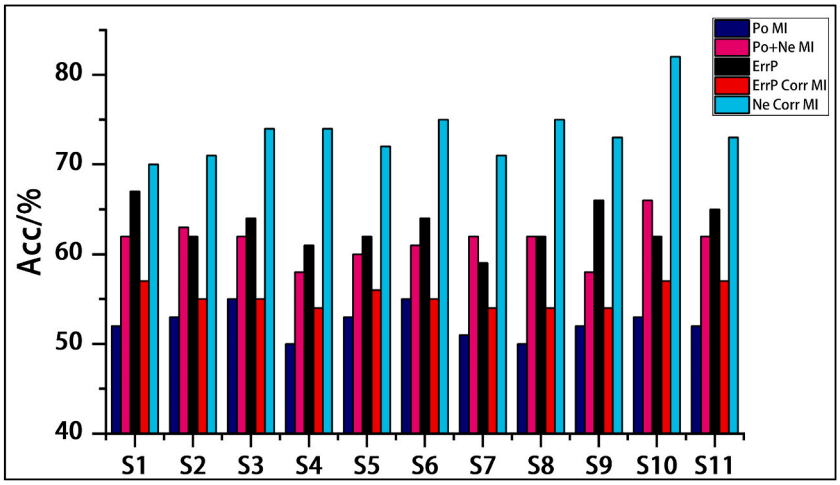


**Fig. 10.** Classification accuracy of different cases of all subjects. In each subject, the average accuracy of Ne Corr MI was significantly higher compared to Po MI, with S10 (Female) being the highest at 82%.

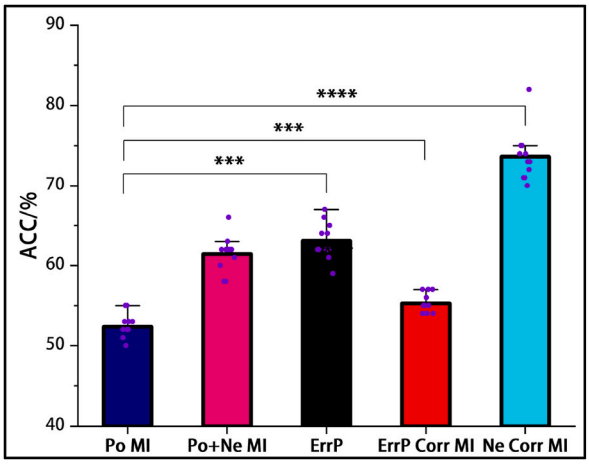


**Fig. 11.** The average accuracy of all subjects. Compared with Po MI, the Ne Corr MI strategy increased by 21.3%, with the largest increase. There were statistically significant differences in the classification results for the five classification cases ($p < 0.0001$).

**Table 3**
Classification accuracy of different metho of all subjects.

| | | S1 | S2 | S3 | S4 | S5 | S6 | S7 | S8 | S9 | S10 | S11 | Average |
|---|---|---|---|---|---|---|---|---|---|---|---|---|---|
| CSP + SVM | Po MI | 43 | 50 | 49 | 49 | 51 | 53 | 53 | [a]55 | 46 | 48 | 52 | 49.9 |
| | ErrP | 51.3 | 62.5 | 31.3 | 48.8 | 33.8 | [a]56.3 | 46.3 | 53.8 | 53.1 | 45.5 | 47.2 | 48.2 |
| FBCSP + SVM | Po MI | 51 | 51 | 50 | [a]56 | 51 | 50 | 56 | 56 | 52 | 55 | 50 | 52.5 |
| | ErrP | 56.3 | 56.3 | 50 | [a]61.3 | 37.5 | 43.8 | 45 | 60 | 53.3 | 58.2 | 54.3 | 52.3 |
| CNN | Po M | 52 | 53 | 55 | 50 | 53 | [a]55 | 51 | 50 | 52 | 53 | 52 | 52.3 |
| | ErrP | [a]67 | 62 | 64 | 61 | 62 | 64 | 59 | 62 | 66 | 62 | 65 | 63.1 |

[a] Represents the highest accuracy for each classification method.).

can be classified into four classes.

The error probability set in this study was 40%. The conclusion drawn by predecessors in the experiment is that the lower the error probability, the greater the potential drop in the ErrP is [6]. It should be noted that different subjects and paradigms may have different peaks, latencies, and durations, so the research on the paradigm proposed in this article can also be carried out from the perspective of error probability. We conducted experiments with subject 3 at three different error rates: 20%, 30%, and 40%. Fig. 12 shows different waves in different error probabilities in FCz of subject 3. At an error rate of 20% (Fig. 12 (a)), the negative wave peak latency of subject 3 was around 250 ms, followed by a distinct positive wave peak, and the ErrP characteristics were consistent with a previous study

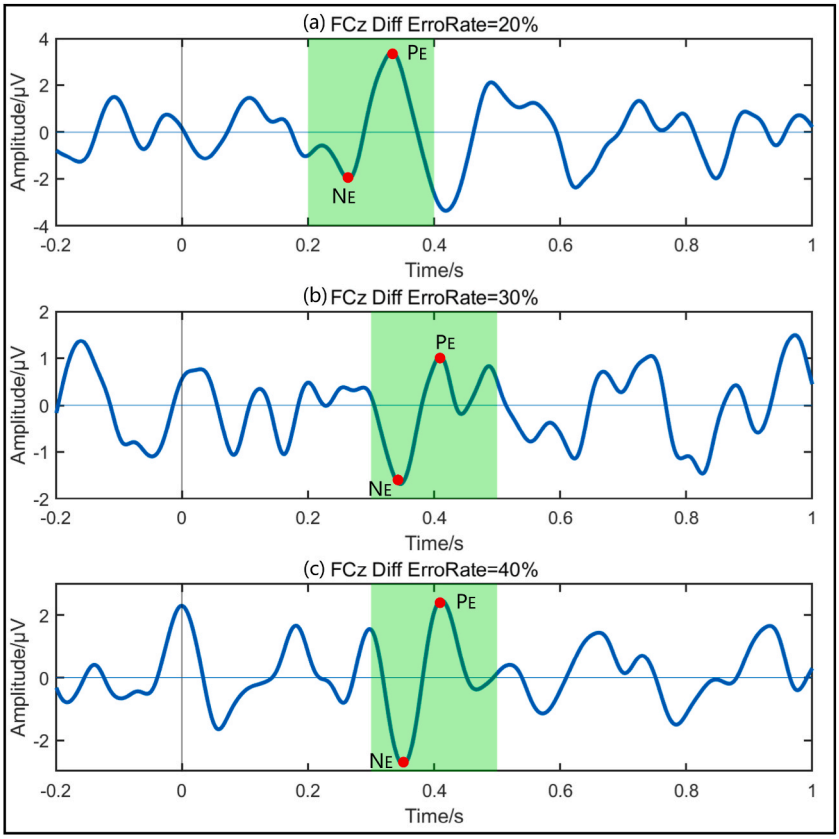


**Fig. 12.** Average difference wave in FCz of different error rates (20% (a), 30% (b), 40% (c)) of subject 3. Time 0 corresponds to the start of image feedback.

[19]. At error rates of 30% (Fig. 12 (b))and 40% (Fig. 12 (c)), the negative crest latency of subject 3 was around 300 ms, with higher error rate conditions producing lower amplitude ErrP, which is consistent with the study [6]. They also reported a decrease in amplitude at higher error rates, which was also found in our experiments, where the positive peak latency of ErrP caused by the condition when the error rate was 40% was lower. We observed that the negative wave had the lowest crest when the error rate was 40%, which is different from previous studies.

For the paradigm proposed in this article, because of its complexity, for a single trial, from the beginning of the cue to the end of the motor imagery task, all of them had a hand-related voice, picture, or video cue, which may cause ERD. As shown in Fig. 13, for the energy change of a single trial in hand open task (Fig. 13 (a)) and hand closed task (Fig. 13 (b)), the occurrence of cross decreased once, followed by a decrease in cue, and then after the picture feedback, there was a decrease, and there was still a decrease during motor imagery. The EEG of the 2–4s image feedback can be considered as action observation (AO). The ERD phenomenon in MI (5–8s) stage is more obvious than that in AO (2–4s) stage, which is consistent with the results of previous studies [34].

In this study, we used ErrP to improve the accuracy of MI and did not show or analyse many features. In the Ne and Po cases, MI ERD has different features. Fig. 14 shows the average ERSP of the C3 electrode in the Ne (Fig. 14 (a) and (b)) and Po cases (Fig. 14 (c) and (d)), where the ERD features in the Ne case are more pronounced, and the frequency band is wider. In the hand-closed MI task (Fig. 14 (a) and (c)), ERD features were more frequently expressed in the high-frequency band above 13 Hz in the Ne task than in the Po task. By contrast, in the hand-open MI task (Fig. 14 (b) and (d)), ERD features in the high-frequency band above 20 Hz were more frequently represented in the Ne task than in the Po task.

To apply this paradigm in real life, it is necessary to consider the error rate, classification accuracy of ErrP, and other factors. Meanwhile, the paradigm still has many other potential research points, such as the MI ERD features in the Ne and Po cases, four-class classification, and the features of MI in the multi-cue case.

It is worth mentioning that the effect of using different brain signals to classify similar movements of the ipsilateral limb differs considerably. Liao et al. achieved 91.28% decoding of complex dexterity functions of fingers in electrocorticogram (ECoG) signals from epileptic patients [10]. The ECoG signal is recorded directly in the cerebral cortex, which possesses a very high spatial resolution and signal quality, and contains a wealth of characteristic information. The ME signal with a high electrode density can also achieve approximately 80% accuracy in decoding similar movements of unilateral limbs after task-specific feature extraction [11], and the motor activation of muscles may provide effective features for classification. However, this classification accuracy is not stable, and the classification accuracy is less than 60% in some tasks [15]. The MI task requires imagining muscle movements with high user fatigue,

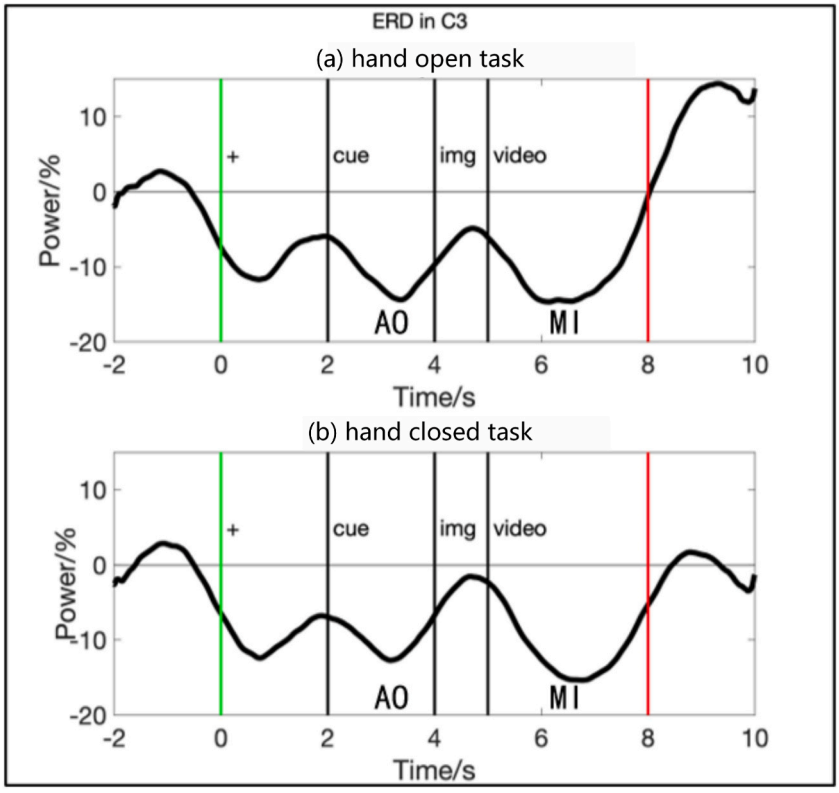


**Fig. 13.** Average MI ERD of subject 1 for hand open task (a) and hand closed task (b) in the C3 channel. Time 0 corresponds to the start of the white cross. 2–4s for AO stage, 5–8s for MI stage.

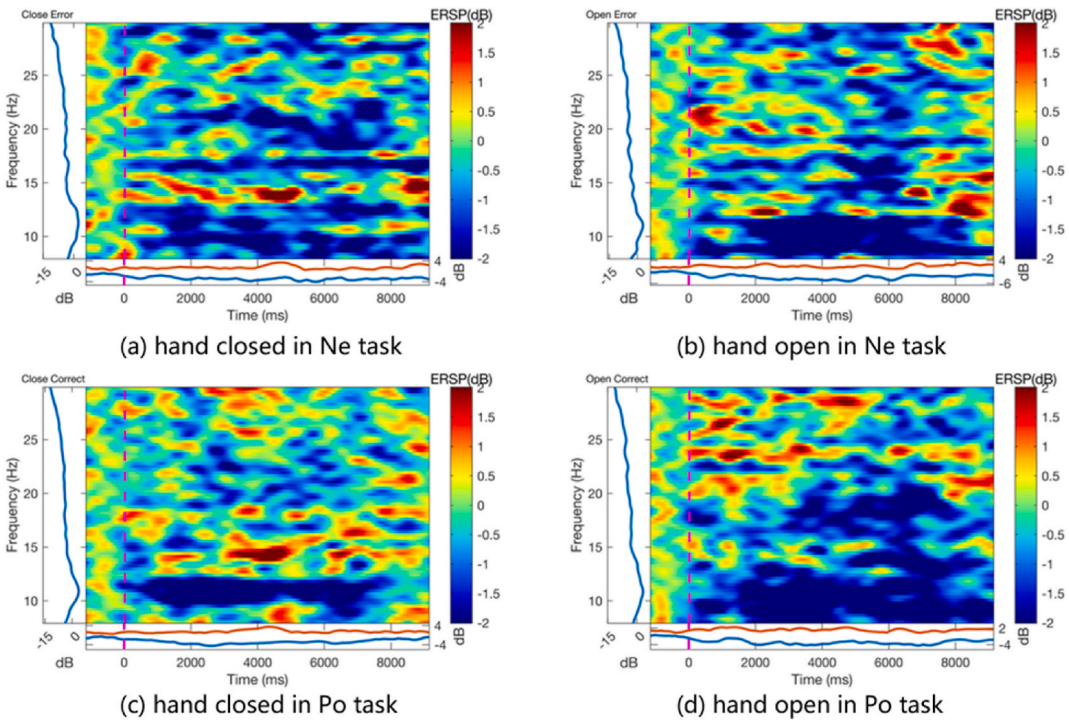


**Fig. 14.** The average ERSP of C3 electrode in Ne and Po tasks for all subjects. Time 0 corresponds to the start of the white cross. The ERD features in the Ne tasks are more pronounced and the frequency band is wider.

and it is impossible to confirm whether the correct imagery is performed according to the given instructions. Combined with the high overlap of brain signals from similar movements of the ipsilateral limb, these difficulties result in a low MI classification accuracy. The hybrid paradigm introduces other physiological measurements into the EEG-BCI paradigm [1]. These signals can add new auxiliary information to MI signal decoding to improve the decoding accuracy.

Because the cortical regions that drive the single-handed open and closed tasks overlap, it is a challenging task to classify both tasks by MI signals. Improving decoding accuracy of similar movements in the same side of the limb allows for more accurate and flexible control of external devices such as mechanical prostheses. It could also lead to better hand rehabilitation for stroke patients. The current dichotomy of different movements of the single-hand is at a random level [14], and multi-category classification is more complex and the classification effect is worse. In this article, we propose a new hybrid paradigm based on MI and ErrP, which can significantly improve the decoding accuracy of hand open and closed actions using simple classification strategies.

This work has some limitations as follows: 1). The accuracy of ErrP is crucial to the effectiveness of the correction strategy. The 60% ErrP detection rate achieved in this article using the CNN method needs to be improved. More in-depth studies to improve the ErrP classification accuracy should be conducted in the future to achieve further development of the application potential of this paradigm. 2). It is meaningful to investigate in depth the decoding of continuous EEG rhythms during action observation, movement imagery, and movement execution in the single-hand open/closed task. In this article, the ERD phenomena of action observation and motor imagery were preliminarily observed in terms of temporal sequence. 3). This article focuses on the improvement of MI classification accuracy by the introduction of ErrP. More sample sizes, feature extraction and classification algorithms should be investigated in the future to get the best classification results. 4). In future research, in addition to this article on hand opening/closing, further exploration can be conducted for the classification of more different hand fine movements to expand the application of the paradigm.

## 5. Conclusion

In this article, we propose a new BCI paradigm that combines the ErrP and MI paradigms. It can simultaneously obtain the features of the ErrP and MI phases in an experiment and can be used to classify EEG signals. The addition of ErrP provided a new feature to the MI paradigm. We used this new feature to improve the MI classification accuracy. The correction strategy can improve the accuracy of MI classification by approximately 20% for single-hand opening and closing. This study contributes to the construction of a BCI system with good classification performance, which can be used for controlling exoskeletons and for rehabilitation training of stroke patients in the future.

## Declarations

This study which involved human subjects was reviewed and approved by the Ethics Committee of Xi'an Jiaotong University (approval number 2021-1577). The participants provided their written informed consent to participate in this study.

## Author contribution statement

Yanghao Lei, Dong Wang: Conceived and designed the experiments; Analyzed and interpreted the data; Wrote the paper, Weizhen Wang, Hao Qu: Performed the experiments, Contributed reagents, materials, analysis tools or data, Jing Wang: Analyzed and interpreted the data; Wrote the paper, Bin Shi: Contributed reagents, materials, analysis tools or data; Wrote the paper.

## Data availability statement

Data will be made available on request.

## Funding statement

This work was supported by the Shenzhen Science and Technology Plan projects under Grant JSGG20201102145602006, and the open project of Henan Key Laboratory of Brain Science and Brain-Computer Interface Technology under Grant HNBBL230101, and 2021 Basic Research Project of Shenzhen Science, Technology and Innovation Commission under Grant JCYJ20210324123414039.

## Additional information

No additional information is available for this paper.

## Declaration of competing interest

The authors declare that they have no known competing financial interests or personal relationships that could have appeared to influence the work reported in this paper.

## References


[1] r. Abiri, s. borhani, E.W. sellers, Y. Jiang, X. Zhao, A comprehensive review of EEG-based brain-computer interface paradigms, J. Neural. Eng. 16 (2019) 1–21.
[2] C. Jeunet, B. Glize, A. Mcgonigal, J.-M. Batail, J.-A. Micoulaud-Franchi, Using EEG-based brain computer interface and neurofeedback targeting sensorimotor rhythms to improve motor skills: theoretical background, applications and prospects, Neurophysiol. Clin. 49 (2019) 125–136.
[3] L.C. Carrere, C.B. Tabernig, Detection of foot motor imagery using the coefficient of determination for neurorehabilitation based on BCI technology, Ifmbe Proceedings 49 (2015) 3188–3193.
[4] A. Kübler, D. Mattia, Brain–computer interface based solutions for end-users with severe communication disorders, The Neurology of Conciousness (2016) 217–240. Second Edition.
[5] C.I. Penaloza, N. Shuichi, BMI control of a third arm for multitasking, Sci. Robot. 3 (2018) eaat1228.
[6] R. Chavarriaga, J. Millan, Learning from EEG error-related potentials in noninvasive brain-computer interfaces, in: IEEE Transactions on Neural Systems & Rehabilitation Engineering A Publication of the IEEE Engineering in Medicine & Biology Society, 18, 2010, p. 381.
[7] T. Liu, G. Huang, N. Jiang, L. Yao, Z. Zhang, Reduce brain computer interface inefficiency by combining sensory motor rhythm and movement-related cortical potential features, J. Neural. Eng. 17 (9pp) (2020), 035003.
[8] L. Yao, N. Mrachacz-Kersting, X. Sheng, X. Zhu, D. Farina, N. Jiang, A multi-class BCI based on somatosensory imagery, IEEE Trans. Neural Syst. Rehabil. Eng. 26 (2018) 1508–1515.
[9] F. Ghani, H. Sultan, D. Anwar, O. Farooq, Y.U. Khan, Classification of wrist movements using EEG signals, J. Next Gener. Infor. Tech.(JNIT) 4 (2013) 29–39.
[10] K. Liao, R. Xiao, J. Gonzalez, D. Lei, Decoding individual finger movements from one hand using human EEG signals, PLoS One 9 (2014), e85192.
[11] J. Deng, J. Yao, J.P.A. Dewald, Classification of the intention to generate a shoulder versus elbow torque by means of a time-frequency synthesized spatial patterns BCI algorithm, J. Neural. Eng. 2 (2005) 131.
[12] J. Zhou, J. Yao, J. Deng, J.P.A. Dewald, EEG-based classification for elbow versus shoulder torque intentions involving stroke subjects, Comput. Biol. Med. 39 (2009) 443–452.
[13] T. Chakraborti, A. Sengupta, D. Banerjee, A. Konar, R. Janarthanan, Implementation of EEG based control of remote robotic systems, in: International Conference on Recent Trends in Information Systems, 2011.
[14] M.M. Ramadhan, S.K. Wijaya, P. Prajitno, Classification of EEG signals from motor imagery of hand grasp movement based on neural network approach, in: IEEE International Conference on Signals and Systems, ICSigSys), 2019, 2019.
[15] A. Vuckovic, F. Sepulveda, Delta band contribution in cue based single trial classification of real and imaginary wrist movements, Med. Biol. Eng. Comput. 46 (2008) 529–539.
[16] Q. Li, Z. Lu, N. Gao, J. Yang, Optimizing the performance of the visual P300-speller through active mental tasks based on color distinction and modulation of task difficulty, Front. Hum. Neurosci. 13 (2019) 130.
[17] Z. Lu, Q. Li, N. Gao, J. Yang, Time-varying networks of ERPs in P300-speller paradigms based on spatially and semantically congruent audiovisual bimodality, J. Neural. Eng. 17 (2020), 046015, 20pp.
[18] M. Falkenstein, J. Hoormann, S. Christ, J. Hohnsbein, ERP components on reaction errors and their functional significance: a tutorial, Biol. Psychol. 51 (2000) 87–107.
[19] R. Chavarriaga, A. Sobolewski, J.D.R. Millán, Errare machinale est: the use of error-related potentials in brain-machine interfaces, Front. Neurosci. 208 (2014).
[20] S. Bhattacharyya, A. Konar, D.N. Tibarewala, Motor imagery, P300 and error-related EEG-based robot arm movement control for rehabilitation purpose, Med. Biol. Eng. Comput. 52 (2014) 1007–1017.
[21] L. Ciabattoni, F. Ferracuti, A. Freddi, S. Iarlori, A. Monteriu, ErrP signals detection for safe navigation of a smart wheelchair, in: IEEE 23rd International Symposium on Consumer Technologies, 2019. ISCT), 2019.
[22] M. Hamedi, S.H. Salleh, A.M. Noor, Electroencephalographic motor imagery brain connectivity analysis for BCI: a review, Neural Comput. 28 (2016) 1–43.
[23] A. Kumar, L. Gao, E. Pirogova, Q. Fang, A review of error-related potential-based brain–computer interfaces for motor impaired people, IEEE Access 7 (2019) 142451–142466.
[24] G. Pfurtscheller, C. Neuper, Future prospects of ERD/ERS in the context of brain-computer interface (BCI) developments, Prog. Brain Res. 159 (2006) 433.
[25] G. Liu, J. Wang, Egg: an analytic brain-computer interface algorithm, IEEE Trans. Neural Syst. Rehabil. Eng. 30 (2022) 643–655.
[26] G. Liu, It may be time to improve the neuron of artificial neural network, TechRxiv (2020).
[27] G. Liu, J. Wang, Dendrite net: a white-box module for classification, regression, and system identification, in: IEEE Trans. Cybern., 2021.
[28] N.S. Kwak, K. Müller, S.W. Lee, A convolutional neural network for steady state visual evoked potential classification under ambulatory environment, PLoS One 12 (2017).
[29] S. Ioffe, C. Szegedy, Batch normalization: accelerating deep network training by reducing internal covariate shift, in: International Conference On Machine Learning, 2015, pp. 448–456. PMLR.
[30] X. Zhang, G. Xu, X. Mou, A. Ravi, N. Jiang, A Convolutional Neural Network for the Detection of Asynchronous Steady State Motion Visual Evoked Potential, IEEE Transactions on Neural Systems and Rehabilitation Engineering, 2019, 1-1.
[31] A. Hekmatmanesh, H. Wu, F. Jamaloo, M. Li, H. Handroos, A combination of CSP-based method with soft margin SVM classifier and generalized RBF kernel for imagery-based brain computer interface applications, Multimed. Tool. Appl. 79 (2020) 17521–17549.
[32] Y. Chu, B. Zhu, X. Zhao, Y. Zhao, Convolutional neural network based on temporal-spatial feature learning for motor imagery electroencephalogram signal decoding, Sheng wu yi xue gong cheng xue za zhi = Journal of biomedical engineering = Shengwu yixue gongchengxue zazhi 38 (2021) 1–9.
[33] P.K. Parashiva, A.P. Vinod, Improving direction decoding accuracy during online motor imagery based brain-computer interface using error-related potentials, Biomed. Signal Process Control 74 (2022).
[34] J.-R. Duann, J.-C. Chiou, A comparison of independent event-related desynchronization responses in motor-related brain areas to movement execution, movement imagery, and movement observation, PLoS One 11 (2016).